Optomechanical Design Principles

Daniel Vukobratovich

2.1 Introduction

Optical engineering is defined as the control of light. Light is controlled by interaction with surfaces, as is the case in refraction or reflection. Optomechanics is defined as that part of optical engineering concerned with maintaining the shape and position of the surfaces of an optical system.

Deviation from a stress-free condition is defined as deflection. Deflection affects the shape and position of surfaces in an optical system. Very small deflections, sometimes as small as one part per million or less, are important in optomechanical engineering. Unlike ordinary mechanical engineering practice, emphasis in design of optomechanical systems is on deflection, or strain, rather than strength, or stress.

This chapter discusses engineering design methods to counteract the effects of deflection on the performance of an optomechanical system. The following topics are covered in this chapter:

1. Service environments
2. Structural design
3. Kinematic design
4. Athermalization
5. Vibration control

2.2 Service Environments

Often the exact service environment of the system is not well understood. To overcome lack of knowledge about the actual working environment for the system, standard environment specifications are used. Military standards are used in the U.S. engineering community as reference environments. One such military standard for environments is Military Standard 810, Environmental Test Methods and Engineering Guidelines.[1] Not all applications require the use of military environmental standards. Systems intended for use in laboratory environments need not accommodate

the very severe specifications typical of military systems. Laboratory environments are normally assumed to be similar to those described in the standards on environment control[2] such as ASHRAE Standard 55-81 and on vibration control.[3] Table 2.1 provides examples of service environments, from mild to severe.

TABLE 2.1   Service Environments

Environment	Normal	Severe	Extreme	Example of Extreme
Low temperature	293 K	222 K	2.4 K	Cryogenic satellite telescope
High temperature	300 K	344 K	423 K	White cell for combustion studies
Low pressure	88 KPa	57 KPa	0	Satellite telescope
High pressure	108 KPa	1 MPa	138 MPa	Submersible window
Humidity	25–75% RH	100% RH	(Underwater)	Submersible window
Acceleration	2 g	12 g	11×10^3 g	Gun-launched projectile
Vibration	200×10^{-6} m/sec RMS, $f \geq 8$ Hz	0.04 g^2/Hz $20 \leq f \leq 100$ Hz	0.13 g^2/Hz $30 \leq f \leq 1500$ Hz	Satellite launch vehicle

2.3 Structural Design

The support structure of an optical system must maintain the position of the optical components relative to each other within design tolerances. The most common load on optical systems is self-weight, due to gravity. Structures with a self-weight deflection that is less than the alignment tolerance are considered stiff. If the self-weight deflection exceeds the alignment tolerances, the optical support structure is compliant.

Conventional definitions of structural efficiency in mechanical engineering are based on strength-to-weight ratios. In contrast, structural efficiency in optomechanical support structures is determined by stiffness-to-weight. Stress in an optomechanical support structure is at a low level in comparison with structures used in other mechanical engineering applications.

One index of structural efficiency for optomechanical support structures is fundamental frequency. Fundamental frequency of a support structure is determined by both stiffness and weight. The fundamental frequency of a structure is a measure of the stiffness-to-weight ratio of a structure. Self-weight deflection is related to fundamental frequency by:[4]

$$f_n = \frac{1}{2\pi} \sqrt{\frac{g}{\delta}}$$

where f_n = the fundamental frequency, in Hz
   g = the acceleration due to the Earth's gravity
   δ = the self-weight deflection of the support structure

Fundamental frequency of a self-weight loaded beam is given by:[5]

$$f_n = \frac{\lambda_i^2}{2\pi L^2} \left(\frac{EI}{m} \right)^{\frac{1}{2}}$$

where f_n = the fundamental frequency, in Hz
   λ_i = a dimensionless constant depending on the type of beam support
   L = the beam length
   E = the elastic modulus of the beam material
    I = the cross-section area moment of inertia of the beam

m = the mass per unit length of the beam

The above equation is more useful if it is expanded to show the relationships between material properties and the geometrical efficiency of the beam shape. In the above equation, the mass per unit length is equivalent to the beam cross section multiplied by the mass density of the beam material. Using this relationship, the above equation for fundamental frequency becomes

$$f_n = \frac{\lambda_i^2}{2\pi L^2}\left(\frac{E}{\rho}\right)^{\frac{1}{2}}\left(\frac{I}{A}\right)^{\frac{1}{2}}$$

where E/ρ = the specific stiffness, the ratio of material elastic modulus to material elastic modulus
I/A = the ratio of area moment of inertia of the beam to cross-section area

The highest fundamental frequency is produced by selecting a material with greatest values of E/ρ and I/A. The ratio E/ρ is a measure of the structural efficiency of the material, while the ratio I/A is a measure of the geometric efficiency of the beam cross section. Efficiency is independent of the strength of the material. There is no reason in optomechanical design to use high-strength materials to provide structural efficiency.

The specific stiffness, or ratio of elastic modulus to density, is of considerable importance in the design of optomechanical support structures. For most common materials, the ratio E/ρ is constant,[6] with a value of about 386×10^{-9} m^{-1}. There are materials such as beryllium and silicon carbide with ratios of E/ρ below this constant. Such materials are considered lightweight materials.

Selection of materials for optomechanical support structures involves a variety of properties other than specific stiffness. Damping capacity, which is a property associated with the dissipation of energy in the material when excited by vibration, is important for dynamic environments. Materials with high damping capacities are often selected for use in optomechanical systems subjected to vibration. Damping capacities of materials are given in Lazan[7] and other references.[8-10] Other material properties of interest are discussed in standard engineering materials selection handbooks. Ashby[11] presents material properties in the form of selection charts. These charts are useful in selecting materials with optimum properties for optomechanical applications.

In cases where the weight of the support structure is limited, efficiency of the support is improved through the use of optimization. An example of the usefulness of optimization is the placement of two simple supports for a beam. Careful selection of the supports substantially reduces beam deflection.

If the beam is of uniform cross section and is carrying a uniform load, the optimum location of the support points to minimize the slope from end to end is at a distance of 0.2222 times the overall length from each end. The maximum slope for a beam supported by two points at this optimum distance is given by:

$$\theta_b = 0.001543\frac{wL^3}{EI}$$

where θ_b = the maximum slope change of the beam
w = the weight per unit length of the beam (self-weight and load)
L = the beam length
E = the elastic modulus of the beam material
I = the area moment of inertia of the beam

If the beam is of uniform cross section and is carrying a uniform load, the optimum location of the support points to minimize the deflection from end to end is at a distance of 0.2232 times

the overall length from each end. The maximum deflection for a beam supported by two points at this optimum distance is given by:

$$\delta_b = 0.0002698 \frac{wL^4}{EI}$$

where δ_b is the maximum deflection from end to end of the beam.

If the beam is of uniform cross section and is carrying a moving load, the location of the two simple supports to minimize the slope is at 0.1189 times the overall beam length from the end. The change in slope for a beam supported by two points at this optimum distance is given by:

$$\theta_m = 0.03727 \frac{WL^2}{EI}$$

where θ_m = the change in slope under the weight of the moving load
W = the weight of the moving load

If the beam is of uniform cross section and is carrying a moving load, the optimum location for the two simple supports to minimize deflection from end to end is at 0.1556 times the overall length of the beam from the end. The maximum change in deflection under the weight of the moving load for a beam on simple supports at these optimum locations is given by:

$$\delta_m = 0.006811 \frac{WL^3}{EI}$$

where δ_m is the change in deflection under the weight of the moving load.

Many optical support structures consist of a beam of uniform cross section with an optical component at each end. A laser cavity is an example of such a structure. Alignment of the optical components at each end is maintained with accuracy through the use of a special category of optimum locations for the beam supports. By placing the two simple supports for the beam at the Airy points, the end slope of both ends of a uniformly loaded beam becomes zero. With both supports at the same distance from the beam ends, and the end slopes equal to zero, the beam ends are in alignment. This alignment is preserved regardless of the orientation of gravity with respect to the beam. The location of the Airy points is at 0.2113 times the overall length of the beam from the ends. This location for the simple supports assumes that the weight of the optical components at each end of the beam is small in comparison with weight of the beam.

If the weight of the optical components at each end of the beam is not small in comparison with the weight of the beam, the location of the two Airy points is found using the following equation:

$$L_s = \frac{L_b}{2}\left(1 - \left[1 - \frac{W_b}{6\left(\frac{W_o}{2} + \frac{W_b}{4}\right)}\right]^{\frac{1}{2}}\right)$$

where L_s = the location of the beam supports from one end of the beam

L_b = the beam length
W_b = the weight of the beam
W_o = the weight of the optics at one end of the beam

In some applications multiple supports are required for a beam. This is a difficult optimization problem; however, in many cases deflection is reduced to a low level through the use of a distributed set of simple supports at the Airy points. The optimum spacing required between two adjacent support points for a uniformly loaded beam to maintain the Airy condition with n simple supports is given by:

$$L_s = \frac{L_b}{\sqrt{n^2 - 1}}$$

where L_s = the spacing between adjacent support points
L_b = the beam length
n = the number of support points

Efficiency of structural connections is often overlooked in the design of optical support structures. A bolted connection designed using normal strength of materials practice typically transmits only about 25% of the moment applied to the connection. Increasing the number of bolts in the connection by a factor of 2 or 3 increases the amount of moment transmitted to about 50%. For maximum stiffness it is desirable to limit the number of connections in a structure. The stiffness of bolted and riveted joints, as well as pin connections, is determined using methods given in Levina[12] and Rivin.[13]

The following types of structural connections are listed in order of decreasing stiffness:

1. Cast or machined from solid ("hog out" construction)
2. Welding
3. Bolting, using maximum number of bolts possible due to geometry ("overbolting")
4. Riveting
5. Conventional bolting
6. Adhesives

In design of an optical support structure, it is not necessary to reduce deflection at all parts of the structure. As shown by the Airy point-supported beam discussed above, deflection of the support structure is acceptable if optical alignment is not affected. The principle of equal and parallel end deflections used in the Airy point-supported beam is extended to a truss through the use of a Serrurier truss.[14] The Serrurier truss consists of a truss supported at its center of gravity, with optical components at each end of the truss. The truss ends remain equal and parallel to each other regardless of the direction of the gravity vector. For equal and parallel deflections of the end rings of the Serrurier truss, the following condition must be satisfied:

$$\frac{w_1}{E_1 A_1}\left(\frac{4L_1^2}{b^2} + 1\right)^{\frac{3}{2}} = \frac{w_2}{E_2 A_2}\left(\frac{4L_2^2}{b^2} + 1\right)^{\frac{3}{2}}$$

where w_1, w_2 = the end ring loads
E_1, E_2 = the elastic modulii of the truss member
A_1, A_2 = the cross-section areas of the truss members
L_1, L_2 = the distances from the center of gravity to the end ring loads
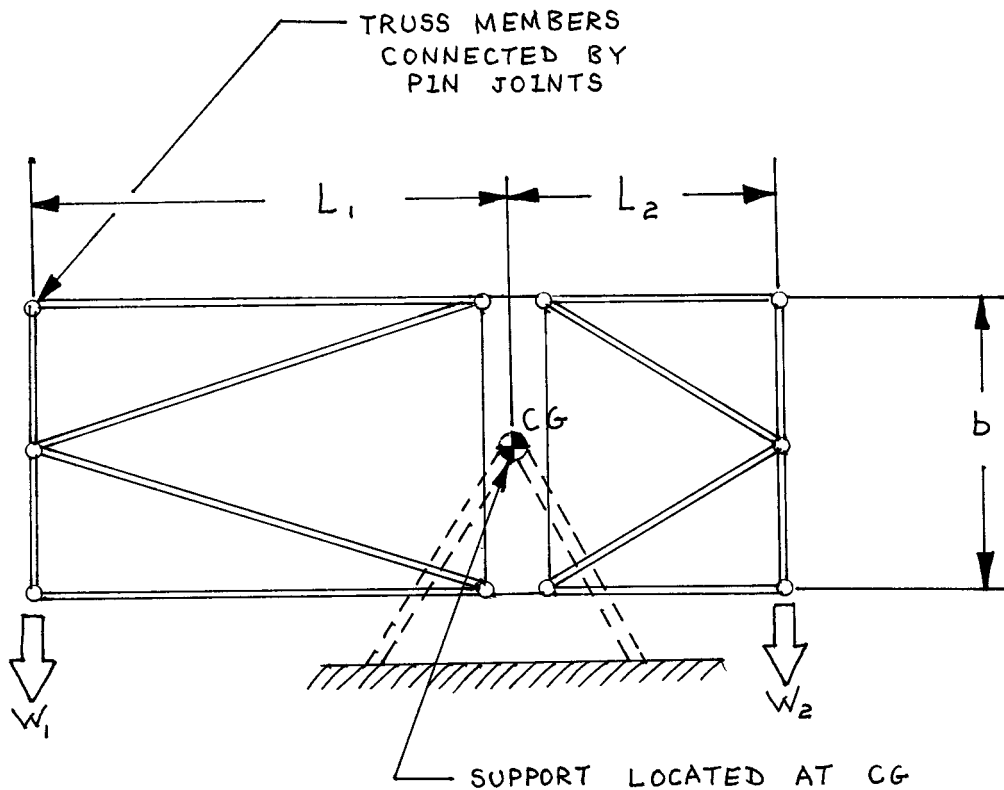b = the end ring diameter

FIGURE 2.1 Serrurier truss geometry.

Figure 2.1 shows a side view of the Serrurier truss geometry. The maximum deflection of either end ring is given by:

$$\delta_{max} = \frac{Wb}{4EA}\left(\frac{4L^2}{b^2} + 1\right)^{\frac{3}{2}}$$

In some cases it is necessary to locate optical components in portions of the structure which experience greater deflection than the allowable alignment tolerance. One possible solution to this problem is an insensitive optical design. Fold mirrors are replaced with penta-prisms which are insensitive to rotation in one plane. Similar in function to penta-prisms are penta-mirror combinations.

For an afocal system, single lens components are replaced by a pair of components, one positive and one negative.[15] The positive and negative components are placed so that the nodal point of the combination lies on the intersection of two lines. One line is a perpendicular to the focal plane of the system. The other line is drawn through the centers of the two components when the structure is undergoing deflection. Locating the nodal point at this intersection produces a rotation of the two-lens combination about its nodal point. Rotation about the nodal point does not cause motion in the final image plane.

For such an insensitive combination, the following equation must be satisfied:

$$f^2 = p(p+s)$$

where   f = the focal length of the afocal component
         p = the location of the rear nodal point, measured from the rear vertex of the second
             lens element
         s = the separation of the two optical elements

The focal lengths f_1 and f_2 of the two optical elements replacing the single lens are given by:

$$f_2 = f\left(\frac{s - f_1}{f - f_1}\right)$$

$$f = \frac{fs^2}{f_1^2} - \frac{s^2}{f_1}$$

Weight relief reduces the self-weight deflection to a very low level. Weight relief is obtained through the use of "off-loading" mechanisms. These mechanisms are soft in all but the direction of the gravity vector. Examples of this type of mechanism include springs, counterweighted levers, air bags, and mercury floats. Weight relief was common prior to the development of high capacity precision bearings. Although not common today for support structures, weight relief is still used for large optical mounts. Air bag support is provided for the primary mirrors of the multiple mirror telescope (MMT) at Mt. Hopkins Observatory.

A simple example of weight relief is the counterweight system used on older refractor telescopes.[16] A lever arm is parallel to the telescope tube and pivoted at the center of gravity of the tube. One end of the pivoted arm is attached to the objective end of the telescope tube, while the other floats free with a counterweight equivalent to the weight of the objective. The lever arm relieves the telescope tube of the weight of the objective, which reduces the deflection of the objective relative to the focal plane. The counterweight location at the other end of the telescope tube moves the center of gravity toward the focal plane, reducing the swing of the eyepiece.

More complex off-loading schemes were developed to reduce the load on precision bearings. Both whiffle tree mechanisms and mercury floats are used for this purpose. The 2.5-m Hooker telescope at Mt. Wilson observatory is provided with a mercury float to reduce the load on the polar axis bearings.[17]

2.4 Kinematic Design

It is desirable to hold optical components in a way that is repeatable and low in stress. The tolerances associated with optical systems require extremely accurate mechanical mounting surfaces to achieve these goals. Such extremely accurate mounting surfaces are very expensive to produce. Kinematic methods provide accurate and repeatable mounting of optical components, in a low stress condition, at much lower costs than conventional precision mechanical methods.[18]

Kinematic methods are derived from the principle of constraint of a rigid body. Every rigid body possesses six degrees of freedom in translation and rotation about each of three mutually perpendicular axes. Perfectly rigid bodies can touch only at infinitely small points. A perfectly rigid body has six N degrees of freedom, where N is the number of contact points.[19] Any rigid body with more than six contact points is overconstrained. An overconstrained rigid body is likely to have an uncertain position and be distorted from its stress-free condition.

The application of kinematic theory consists of selecting no more than six contact points to provide the type of support or motion required. Kinematic supports with less than six contact points permit motion of the supported body. The motion is a "degree of freedom" and is correlated with the number and geometry of the support points.

Real kinematic mounts violate the assumption of an infinite elastic modulus associated with a rigid body. Kinematic designs attempt to approximate the ideal point contact through the use of Hertz contact. In a Hertz contact, the bodies are assumed to be ellipsoidal, with differing radii of curvature. The area of contact developed is due to the radii of the contacting solids, the force pushing the solids into contact, and the elastic properties of the materials.[20] Approximate methods are used to calculate the deflection and stress developed in the Hertz contacts associated with kinematic design.[21]

The simplest type of kinematic mount is used to fix the location of a body. This requires six contact points. Often illustrated in texts on instrument design is the "Kelvin clamp".[22] The Kelvin clamp employs three spherical locating features attached to the body. One spherical feature is located in a trihedral socket, one in a v-groove, and one is placed on a flat. There is one contact point for each flat surface in contact with a sphere: three for the trihedral contact, two for the v-groove, and one for the flat. Six contact points uniquely locate the body without overconstraint.

Although theoretically attractive, the Kelvin clamp is not a physically practical design due to the difficulty of making trihedral sockets. One method of producing three-point contact between a sphere and socket replaces the trihedral socket with a compound socket. The compound socket consists of three spheres forced into a common cylindrical hole or socket.[23] The locating spherical feature rests against the three spheres. Another method is the replacement of the trihedral socket with a conical socket. A conical socket is readily produced, but is not truly kinematic since line contact develops between the conical surface and spherical locating feature.

An alternate to the Kelvin clamp is the three-groove kinematic mounting or coupling.[24] The three-groove kinematic coupling retains the spherical locating features attached to the body. In place of the socket, v-groove and plane of the Kelvin clamp are three v-grooves. Each v-groove provides two points of contact. In a planar assembly, the long axes of the three v-grooves intersect at a common point and are about 120° apart. Figure 2.2 shows a typical three v-groove kinematic coupling. Three-dimensional configurations are also possible.[25]

Guidance of motion is provided by use of kinematic principles without any play or backlash. Use of kinematic design provides unique location of the body at all times, with a resulting absence of lost motion in all but the desired direction. Both translation and rotation are possible in kinematic designs.

A kinematic linear translation guiding mechanism consists of two parallel cylinders in contact, forming a "v-groove" and an adjacent flat guide way. There are three hemispherical feet located below and attached to the moving carriage. Two of the hemispheres ride in the trough formed by the two cylinders in contact. Each hemisphere makes a contact with each cylinder, so there are four contacts between the two cylinders and hemispheres. The third hemisphere is in contact with the flat guide way, providing a fifth contact point. There are 6-N remaining degrees of freedom. The number of contact points, N, is equal to 5. Linear translation, in the direction of the axis of the trough formed between the two cylinders, is this degree of freedom.

Rotation and translation are provided in a single kinematic mechanism by placing a cylinder between two sets of adjacent cones. There are four contact points between the cylindrical surface and the four conical surfaces. Rotation of the cylinder about its axis is possible, as is linear translation of the cylinder along its long axis. This type of mount is used to support alignment telescopes and collimators.

Pure rotation is obtained in the above example by adding a fifth contact point. This contact point is a hemisphere bearing against the flat end of the cylinder. Alternate kinematic rotation guides use curved tracks or combinations of cylindrical and conical ended shafts. A variety of kinematic mechanisms are possible for guiding motion.[26]

A serious limitation on the use of kinematic design is stress in the elastic contacts. Hertz contact stress between curving surfaces is usually much higher than the usual stresses in a support structure. The high stress level associated with the elastic contacts in kinematic design often lead to the use of hard, high strength materials such as sapphire and tungsten carbide. Rapid wear in the area of the elastic contact is a potential problem associated with kinematic guides. Potential wear is assessed
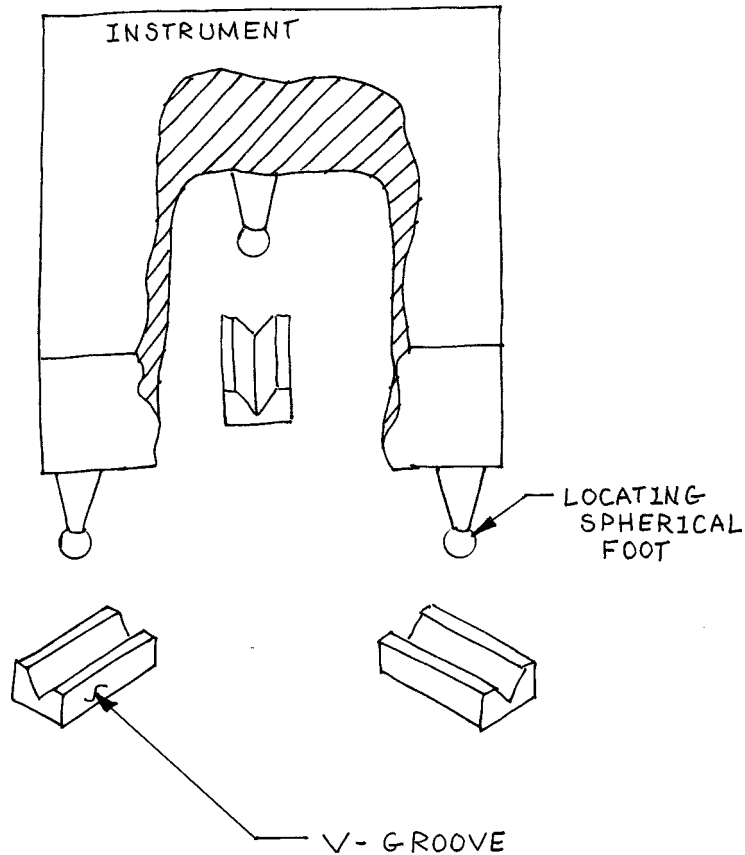
FIGURE 2.2 Kinematic coupling.

using the contact stress models developed by Bayer.[27] Wear is reduced to "zero" using the IBM zero wear theory.[28] This wear model states that zero wear is defined as wear equivalent to the surface finish of a polished metal part. Zero wear occurs when:

$$\frac{\tau_{max}}{\tau_{ys}} \leq 0.2$$

where τ_{max} = the maximum shear stress in the elastic contact
       τ_{ys} = the yield stress in shear of the material

Semi-kinematic design reduces the elastic contact stress by replacing the point contacts of a true semi-kinematic design with small contact areas. These areas are sized to reduce the stress to acceptable levels. Semi-kinematic design also provides for increasing the number of supports without overconstraint. Increasing the number of supports is sometimes necessary to decrease self-weight deflection or to improve stiffness.

In semi-kinematic design, supports are located using kinematic theory. Each support point in the kinematic design is replaced with a small contact area. Errors in the fit between the two surfaces in contact at each support induces moments in the supported body. Successful semi-kinematic design requires careful attention to the quality of the support areas to minimize the support-induced moments.

There are two methods for providing high quality support areas in semi-kinematic design: tight tolerances on the surfaces, and surfaces with rotational compliance. Semi-kinematic mounts are

used in supporting optics during diamond turning. In this application the tolerances of the mounting surfaces must be comparable to the tolerances of the optical surface. This condition is obtained in diamond turning of optics, but is difficult to provide for most other applications. A more reasonable tolerance is that the flatness and co-planarity of the mounting surfaces must be less than the elastic deflection of the mounting surface. For most applications, even this tolerance is well below what is normally obtained with conventional production methods.

An alternative to tight tolerances is to introduce rotational compliance into the mounting surface. This is common in the design of tooling fixtures. One commercial component that is used for semi-kinematic mounts is the tooling (spherical) washer set. A tooling washer set consists of a concave and convex set of mating washers, with an oversized central hole. During assembly the washers tilt and de-center to reduce induced moments in the part.

A sphere in cone geometry is used for semi-kinematic mounts. A line contact develops between the sphere and cone. For optimum performance, the profile error on the conical surface must be comparable to the profile error (roundness) of the sphere. Trylinski[29] gives equations for calculating the stress and residual moment for a sphere in a conical socket:

$$\sigma_a = \frac{1}{\pi r}\left[\frac{F_a}{(\sin 2\theta)\left(\dfrac{1-v_s^2}{E_s}\right)+\left(\dfrac{1-v_c^2}{E_c}\right)}\right]^{\frac{1}{2}}$$

$$T_a = F_a \mu r \cos\theta$$

$$\tau_t = \frac{1}{\pi r \cos\theta}\left[\frac{2.5 F_t}{\left(\dfrac{1-v_s^2}{E_s}\right)+\left(\dfrac{1-v_c^2}{E_c}\right)}\right]^{\frac{1}{2}}$$

$$T_t = F_t \mu r$$

where F_a = the axial force acting on the socket
F_t = the shear force acting on the socket
σ_a = the stress due to the axial force
τ_t = the stress due to the shear force
 r = the radius of the sphere
θ = the vertex angle of the conical socket
E_s = the elastic modulus of the sphere
E_c = the elastic modulus of the conical socket
v_s = the Poisson's ratio of the sphere
v_c = the Poisson's ratio of the conical socket
μ = the coefficient of breakaway friction between sphere and conical socket
T_a = the maximum moment due to the axial force
T_t = the maximum moment due to the shear force

Semi-kinematic design is used to provide for multiple point support of bodies without causing overconstraint. Multiple support points are tied together in groups; each group acts as a single kinematic support. The support points in a group are connected by pivots, with each pivot located at the center of gravity of the support points. Residual moments induced in the mounted body using a whiffle tree mechanism arise from friction in the pivots. It is desirable to reduce the pivot friction to a very low level. Since the pivots provide rotation to balance forces, static friction is important.

The simplest example of a whiffle tree is a support for a beam. Each of the two simple supports for the beam is provided with a rocker. At each end of the rockers is a contact point with the bottom of the beam, so there are four points in contact with the beam. This type of mechanism is self-adjusting for irregularity in the beam.

More complex whiffle trees are created by adding pivots to the ends of the balance beam carrying subrockers. The whiffle tree is cascaded using the approach to provide 8, 16, or more support points. Performance of the whiffle tree is determined by the number of supports, pivot friction, and rocker stiffness. The distance between adjacent support points in a whiffle tree for a uniformly loaded beam is determined using the Airy point equation given above. Figure 2.3 shows a typical whiffle tree design for a beam.
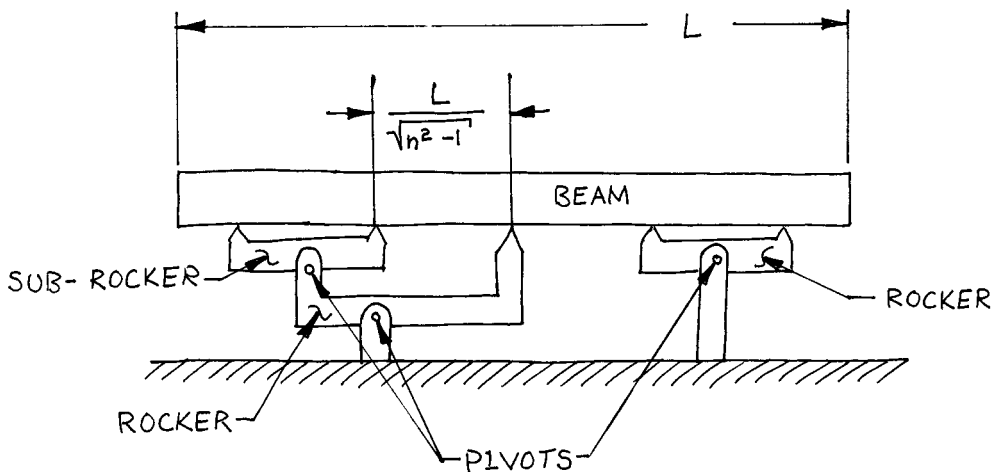

FIGURE 2.3 Whiffle tree-supported beam.

A similar approach is used in whiffle trees supporting plates. In this application, the pivots are attached to subplates and provide rotation about two different axes. The subplates are normally triangular, with contacts at the tips of the triangles. The simplest type of plate support uses three pivots below the plate, located using kinematic principles. Each pivot carries a triangular rocker plate with three contact points. The optimum location for the support points is determined using complex structural analysis methods. Alternately, the support points are located using the principle of equal areas. Each support point carries the same plate area and is located at the centroid of the area. In axisymmetric plates (optical mirrors) the support points in the whiffle tree are equally spaced on concentric rings.

2.5 Athermalization

There are three types of thermal effects on optomechanical systems:

1. A temperature change induces distortion in the optical element due to the material properties of the element. Important thermal properties determining the amount of distortion

are the thermal coefficient of expansion (α), spatial variation in thermal coefficient of expansion ($\Delta\alpha$), thermal distortion index (ratio of thermal coefficient of expansion to thermal conductivity, α/k), and thermal diffusivity (D).

2. A temperature change induces distortion in the optical element due to the way in which the element is mounted. This distortion is due primarily to the difference in thermal coefficients of expansion of the mount and optical element materials. This type of thermal distortion is discussed in the section on optical mounts.

3. A temperature change induces distortion in the optical support structure. Distortion of the optical support structure causes a loss of optical alignment. The most important effect of this loss of alignment is a change in system focus. Athermalization means that the optical system maintains focus when the temperature changes.

A window is a zero power optical component used in transmission. Windows provide an introduction to optical effects of temperature changes. Consider a circular, plane parallel window subjected to a linear temperature gradient through its thickness (linear axial gradient). The hot side of the window expands relative to the cold side. The change in area of the two sides of the window causes the window to spring out of shape and become curved. Since the surfaces are curved, the window acts as a meniscus lens with a power (power is defined as the reciprocal of the focal length) given by[30,31]

$$\frac{1}{f} = \frac{n-1}{n}\left(\frac{\alpha}{k}\right)^2 hq^2$$

where $1/f$ = the power of the distorted window
        n = the index of refraction of the window material
        α = the thermal coefficient of expansion of the window material
        k = the thermal conductivity of the window material
        h = the axial thickness of the window
        q = the heat flux per unit area absorbed by the window

Distortion of a window due to axial temperature gradients is a weak effect. More serious is a radial gradient. The radial temperature profile of a window is determined by heat transfer at the window surfaces. Heat transfer occurs due to conduction, convection, and radiation. Complex temperature profiles develop due to different kinds of heat transfer occurring simultaneously.

A parabolic radial temperature distribution is a good approximation of many types of window heat transfer.[32] The power of a window with a parabolic radial temperature profile is given by:[33,34]

$$\frac{1}{f} = 8\frac{h}{D^2}\Delta T\left[(n-1)(1+v)\alpha + \frac{dn}{dT}\right]$$

where $1/f$ = the power of the distorted window
        h = the window axial thickness
        D = the window diameter
        ΔT = the radial difference in temperature, from center to edge
        n = the index of refraction of the window material
        v = the Poisson's ratio of the window material
        α = the thermal coefficient of expansion of the window material
        dn/dT = the thermoptic coefficient of the window material (change in index of refraction with temperature)

In most applications the effects of radial gradients are much larger than those due to axial gradients. It is desirable to reduce radial temperature differences in optical elements to limit such effects due to gradient. The size of the gradient is reduced by insulating the edge of the window. Titanium is a good material for this application. The thermal conductivity of titanium is much lower than that of most common metals, limiting heat transfer into the mount. In addition, the thermal coefficient of expansion of titanium is a good match with that of many optical materials. An alternate method is heating or cooling the edge of the window to reduce heat transfer. In some cases the radial profile is represented by a polynomial expression of order greater than three. The temperature change associated with this type of gradient is most rapid near the edge of the window. Making the window oversize with respect to the optical clear aperture limits the effect of such higher-order gradients. As a rule of thumb, the window should be about 25% larger in diameter than the optical clear aperture.

The index of refraction of a lens changes with temperature. This change in temperature is due to the thermoptic property ("dn/dT") of the lens material. A change in index of refraction of the lens alters the focal length of the lens. The change in lens focal length with temperature is given by:[35]

$$\beta = \left(\frac{1}{f}\right)\left(\frac{df}{dT}\right) = \alpha - \left(\frac{1}{n - n_{air}}\right)\left(\frac{dn}{dT} - n\frac{dn_{air}}{dT}\right)$$

where
β = the optothermal expansion coefficient
f = the lens focal length
df/dT = the change in lens focal length with temperature
α = the lens material thermal coefficient of expansion
n = the lens material refractive index
n_{air} = the index of refraction of air
dn/dT = the lens material thermoptic coefficient
dn_{air}/dT = the thermoptic coefficient of air

For ordinary optical glass used in visible wavelengths, $n_{air} \approx 1$ and $dn_{air}/dT \approx 0$, so the above equation becomes

$$\beta \approx \alpha - \left(\frac{1}{n-1}\right)\left(\frac{dn}{dT}\right)$$

The above equation indicates that β, the change in lens power with temperature, is a material property and is independent of lens surface curvature. Below is a table (Table 2.2) of the optothermal expansion coefficients, β, of a variety of materials.

TABLE 2.2   Optothermal Expansion Coefficients

Glass Type	β (m/m-k $\times$ 10^{-6})
TiF6	20.94
BK1	3.28
LaKN9	0.32
BAK4	−0.23
KzFS1	−2.89
ZnSe	−28.24
Silicon	−64.10
Germanium	−85.19

In optical systems with multiple lens elements, the optothermal expansion coefficient of the system, β_S, is given by the following equation:

$$\beta_s = \sum_{i=1}^{n} \frac{K_i}{K_s} \beta_i$$

where β_s = the system optothermal expansion coefficient
K_i = the individual element power (reciprocal of focal length)
K_s = the system power
β_i = the individual element optothermal expansion coefficient

For athermalization, the focus of the system must not change with temperature. This condition is obtained if the optothermal expansion coefficient, which represents the change in focus with temperature, is the same as the thermal expansion coefficient of the system. Or

$$\beta_s = \alpha_s$$

The range of thermal expansion coefficients is limited by the availability of adequate materials for optical support structures. It is rare for the optothermal expansion coefficient to be nearly the same as that of a common structural material. It is possible to adjust the optical design of the system to produce a β_s that is the same as a selected thermal coefficient of expansion.

Another structural technique for athermalization is a bi-metallic compensator. A bi-metallic compensator is made of materials with different thermal coefficients of expansion. By adjustment of the lengths of the two types of materials, a good match between the effective thermal coefficient of expansion of the structure along the optical axis and the optothermal expansion coefficient of the structure is obtained. For athermalization using a bi-metallic compensator:

$$\alpha_1 L_1 + \alpha_2 L_2 = \beta_s f$$

where α_1, α_2 = the thermal coefficients of expansion of the two materials in the bi-metallic structure
L_1, L_2 = the respective lengths of the two materials in the bi-metallic structure
β_s = the system optothermal expansion coefficient
f = the system focal length

Figure 2.4 shows two types of bi-metallic compensators. Below is a table (Table 2.3) of some bi-metallic compensator combinations for different types of lens materials:

If the optothermal expansion coefficient of the system is small, a metering structure is used to athermalize the system. A metering structure consists of a structure made of conventional materials that provides stiffness in location in all directions except along the optical axis, and an inner, low thermal coefficient of expansion structure that maintains spacing and alignment with temperature. Typically, the inner structure consists of rods made of a low thermal coefficient of expansion material such as invar. The rods are attached to the optical components and are connected to the optical support structure by linear translation bearings. Low thermal coefficient of expansion materials such as invar often are expensive and low in structural efficiency.[36,37] Metering structures avoid these disadvantages.

Methods used to athermalize reflective systems are similar in some respects to those used for refractive systems. Like lenses, mirrors are sensitive to temperature gradients. A linear axial temperature gradient in a mirror along the optical axis will cause the optical surface of the mirror to change its radius of curvature. The change in surface curvature is determined by the same material
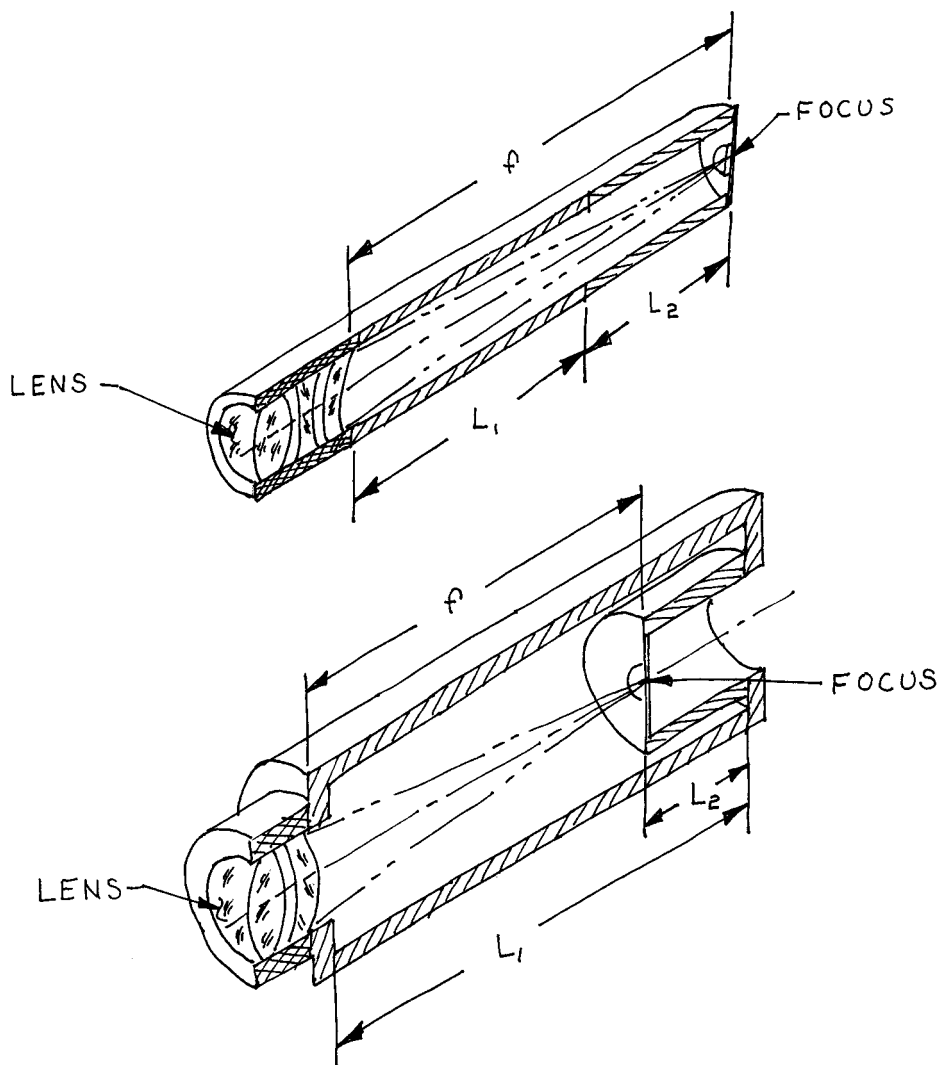
FIGURE 2.4 Bi-metallic compensators. The upper design provides a low effective structural thermal coefficient of expansion and the lower design provides a near-zero to negative effective structural thermal coefficient of expansion.

TABLE 2.3 Bi-Metallic Compensators

Glass Type	β_S (m/m-k × 10⁻⁶)	Material 1	α_1 (m/m-k × 10⁻⁶)	$L_1 \times f$	Material 2	α_2 (m/m-k × 10⁻⁶)	$L_2 \times f$
TiF6	20.94	Aluminum	23	0.678	Stainless steel	16.6	0.322
BK1	3.28	Invar	0.54	0.829	Stainless steel	16.6	0.171
LaKN9	0.32	Invar	0.54	1.01	Aluminum	23	−0.01
BAK4	−0.23	Invar	0.54	1.034	Aluminum	23	−0.034
KzFS1	−2.89	Invar	0.54	1.153	Aluminum	23	−0.153
ZnSe	−28.24	Stainless steel	16.6	1.233	Plastic (ABS) (polyurethane)	209	−0.233
Silicon	−64.10	Stainless steel	16.6	1.419	Plastic (ABS) (polyurethane)	209	−0.419
Germanium	−85.19	Stainless steel	16.6	1.358	Plastic (polyethylene)	301	−0.358

property, the thermal distortion index, that determines the change for a refractive component. The change in surface curvature of a mirror subjected to a linear axial temperature gradient is given by:

$$\frac{1}{R_o} - \frac{1}{R} = \frac{\alpha}{k}q$$

where R_o = the original surface radius of curvature
        R = the radius of curvature of the surface due to the gradient
        α = the thermal coefficient of expansion of the mirror
        k = the thermal conductivity of the mirror material
        q = the heat flux per unit area through the mirror

Analysis of the effects of more complex gradients requires the use of a method developed by Pearson and Stepp.[38] This set of equations provides a means of evaluating the effect of a global temperature change as well as linear temperature gradients. The linear temperature gradients are assumed to lie along each axis of a Cartesian coordinate system, with the origin of the coordinate system at the vertex of the mirror, with the z axis coincident with the optical axis. These equations are applicable for both concave and convex mirrors. For convex mirrors a sign change is necessary. The temperature distribution in the mirror is given by:

$$T(x, y, z) = c_o + c_1(x) + c_2(y) + c_3(z)$$

where c_o = the global change in temperature of the mirror
        c_1 = the linear temperature gradient along the x axis
        c_2 = the linear temperature gradient along the y axis
        c_3 = the linear temperature gradient along the z axis (the optical axis)

The surface deformations due to the above gradients are given by:

$$W(r, \theta) = \frac{\alpha c_3}{8R^2} r^4 \quad \text{(spherical)}$$

$$+ \frac{\alpha c_1}{2R} r^3 \cos\theta + \frac{\alpha c_2}{2R} r^3 \sin\theta \quad \text{(coma)}$$

$$+ \left(\frac{\alpha c_3 h}{2R} - \frac{\alpha c_3}{2} + \frac{\alpha c_o}{2R} \right) r^2 \quad \text{(focus)}$$

$$+ \alpha c_1 h \cos\theta + \alpha c_2 h \sin\theta \quad \text{(tilt)}$$

$$+ \frac{\alpha c_3 h^2}{2} + \alpha c_0 h \quad \text{(piston)}$$

where r = the radius position on the mirror surface
        θ = the angular position on the mirror surface
        α = the mirror material thermal coefficient of expansion
        R = the optical radius of curvature of the mirror surface
        h = the mirror axial thickness

The above equations suggest that temperature gradients are the source of potential problems in mirrors. A mirror exposed to a sudden change in temperature is likely to develop temperature

gradients from its surface to interior. The time required for the mirror to reach thermal equilibrium is estimated using a simple one-degree-of-freedom model. This model gives the time required for the mirror interior to approach the surface temperature after an instantaneous temperature change. The mirror interior temperature after some time is given by:

$$T' \approx T - \Delta T \exp\left(-\frac{\pi^2 D t}{h^2}\right)$$

where T' = the temperature of the mirror after some time t
   T = the initial mirror temperature
   ΔT = the temperature change at the mirror surface
   t = the time after the sudden temperature change
   h = the mirror axial thickness
   D = the thermal diffusivity of the mirror material, where:

$$D = \frac{k}{\rho c_\rho}$$

   k = the thermal conductivity of the mirror material
   ρ = the mirror material density
   c_ρ = the mirror material specific heat

   If the thermal coefficient of expansion of the mirror material is not uniform, the mirror distorts when the temperature is changed. This effect occurs even if the temperature changes globally without any gradients, and is due to the spatial variation of properties in the mirror. As a rule of thumb, a spatial variation of 3 to 5% of the thermal coefficient of expansion should be expected in most materials.[39] Low thermal coefficient of expansion materials, with an α near zero, are less affected by this spatial variation. There may be difficulties due to spatial variation of α with high thermal coefficient of expansion materials (such as aluminum and beryllium) used for mirror substrates. If the mirror thermal coefficient of expansion varies linearly along the axis of the mirror, the surface deformation is given by:

$$\delta = \frac{r^2}{2h} \Delta T \ \Delta\alpha$$

If the mirror thermal coefficient of expansion varies linearly across the diameter of the mirror, the surface deformation is given by:

$$\delta = \frac{r^2}{4h} \Delta T \ \Delta\alpha$$

where in the above equations:

   δ = the surface deformation
   r = the mirror radius
   h = the mirror axial thickness
   ΔT = the change in temperature
   $\Delta\alpha$ = the spatial variation in thermal coefficient of expansion

Making all components, optical and structural, of a system out of the same material is an important method of athermalization of reflective optical systems. This method of athermalization is called "same material athermalization". Although all-glass optical systems have been built,[40] such systems are expensive and fragile. Same material athermalization is commonly used with metal optics. Cost and strength of metal optics and structure are not as much an issue as when glass is used. Cryogenic optical systems often employ same material athermalization.[41,42]

2.6 Vibration Control

Vibration is a source of performance degradation in optomechanical systems. Very low levels of vibration induce a blur in the focus. This vibration-induced blur is sometimes mistaken for blur due to a system misalignment, or an out-of-focus condition. Higher levels of vibration create a time-variant blur, which is at least easy to diagnose. Very high levels of vibration carry the potential for structural failure of the system. In general, operation is not expected at such levels, only survival.

There are two important types of vibration that affect optomechanical systems: periodic and random. Periodic vibration is characterized by a period and amplitude. The amplitude of complex periodic vibration is characterized, statistically, by quantities such as the root-mean-square of the amplitude. Random vibration is also characterized by statistical methods. Random vibration contains all frequencies. One statistical quantity that is often used to describe random vibration is the power spectral density (PSD). The PSD is a measure of the amplitude of vibration contained within some bandwidth, typically 1 Hz. Since PSD is a measure of the area under a curve, it is given in units of area per bandwidth. One such measure is "g^2/Hz", where "g" is a dimensionless acceleration unit (1 g = acceleration of Earth's surface gravity).

Response of systems to vibration is a complex topic. Considerable insight is derived from the use of a simple, single-degree-of-freedom (SDOF) model. This model is used to determine response of systems to both periodic and random vibration. The most important property of a system exposed to vibration is the natural frequency. The natural frequency of a system is that frequency at which the system will oscillate if perturbed from equilibrium. For a simple SDOF system, the fundamental frequency is given by:

$$f_n = \frac{1}{2\pi}\sqrt{\frac{k}{m}}$$

where f_n = the natural frequency, in Hz
  k = the system spring stiffness
  m = the system mass

Many optomechanical systems are mounted kinematically. Certain types of athermalized kinematic mounts employ flexural elements between the optical component and the structure. These flexures act as springs and reduce the fundamental frequency of the mounted component. For athermalization the flexures are compliant in the radial direction and stiff in all other directions. In this case the stiffness of the mounted optic in the radial direction is given by:

$$k_r = \frac{n}{2}\left(k_{rf} + k_{tf}\right)$$

And the stiffness of the mounted optic in the axial direction is given by:

$$k_a = nk_{af}$$

where k_r = the radial stiffness
        n = the number of mounting flexures
        k_{rf} = the radial stiffness of an individual flexure
        k_{tf} = the tangential stiffness of an individual flexure
        k_a = the axial stiffness
        k_{af} = the axial stiffness of an individual flexure

If a system is perturbed from equilibrium, the amplitude of each successive cycle of vibration is less than that of the preceding cycle. This decrease in amplitude of vibration with time is due to energy lost during each cycle. The process of energy loss in a vibrating system is called damping. A system is said to be critically damped if there is no vibration when the system is perturbed from equilibrium. For a SDOF system, the critical damping coefficient C_c is given by:

$$C_c = 2(km)^{1/2}$$

where k = the stiffness
        m = the mass

Real systems are usually not critically damped. It is common to give the system damping in terms of the critical damping ratio. The critical damping ratio C_R is the ratio of the system damping to the amount of damping necessary to make the system critically damped, or C/C_c. The critical damping ratio is a dimensionless number, but is usually given as a percentage. The critical damping ratio of optomechanical systems is often less than 5%.[43]

The response of a SDOF system to a sinusoidal excitation is given by:

$$\frac{X_0}{X_1} = \left[\frac{1 + 2\frac{f}{f_n}c_R}{\left(1 - \frac{f^2}{f_n^2}\right)^2 + \left(2\frac{f}{f_n}c_R\right)^2} \right]^{\frac{1}{2}}$$

where X_0 = the amplitude of oscillation of the SDOF system
        X_1 = the amplitude of oscillation of the exciting force
        f = the frequency of the exciting force
        f_n = the natural frequency of the SDOF system
        c_R = the critical damping ratio of the SDOF system

There are three special cases of the above equation: spring, damper, and mass-controlled cases. In the mass-controlled case, the fundamental frequency is much less than the frequency of excitation ($f \gg f_n$). The response is determined by the amount of mass of the system and the frequency ratio. In the damper-controlled case, the fundamental frequency is near the frequency of excitation ($f \cong f_n$), and the response is determined by the amount of damping in the system. In the spring-controlled case, the fundamental frequency is much greater than the frequency of excitation ($f \ll f_n$), and the response if determined by the spring stiffness of the system.

The ratio of X_0/X_1 is the transmissibility of the system and is a dimensionless number. A transmissibility of less than unity means that the amplitude of response of the SDOF system is less than the exciting force amplitude. Transmissibilities of greater than unity mean that the amplitude of response of the SDOF system is greater than the exciting force amplitude. A transmissibility of greater than unity is very undesirable in optomechanical systems. The Q of a system is the transmissibility at resonance.

A vibration isolation system operates in the mass-controlled domain, where the frequency of excitation is always at least $\sqrt{2}$ higher than that of the fundamental frequency of the isolation system.[44] In the mass-controlled case, the transmissibility T ($T = X_0/X_1$) is given approximately by:

$$T = \frac{X_0}{X_1} \approx \left(\frac{f_n}{f}\right)^2$$

where   T = the transmissibility
        X_0 = the amplitude of oscillation of the SDOF system
        X_1 = the amplitude of oscillation of the exciting force
        f = the frequency of the exciting force
        f_n = the natural frequency of the SDOF system

At high frequency ratios, the above equation indicates that transmissibility is small. For example, a typical vertical fundamental frequency for an isolation system is 2 Hz. If this isolation system is subjected to a 60-Hz excitation, the transmissibility is about 0.001. At low frequency ratios, the transmissibility will approach unity, and isolation suffers. Damping increases the transmissibility of an isolation system at high frequency ratios and is, therefore, undesirable. Some damping is necessary to prevent damage to the isolation system if exposed to excitation at the natural frequency of the system. Nonlinear damping response is provided in isolation system through the use of surge tanks connected to the cylinders of air springs by metering orifices. Near resonance, the surge tank damped air spring is high in damping, and response is limited. At high frequencies, the surge tank is not effective in damping and the air spring isolator operates as though it were undamped.[45]

Isolation systems consist of a stiff platform supported on isolators. Platform stiffness is much higher than that of the isolators. Due to the high platform stiffness, the fundamental frequency of the isolation system is determined by combining the stiffness of the independent isolators with the inertial properties of the isolators. An isolation system has three natural frequencies in translation, one in each axis, and three natural frequencies in rotation, one about each axis. Natural frequencies of the isolation system in translation and rotation are given by:[46]

$$f_{nt} = \frac{1}{2\pi}\left(\frac{1}{m}\sum_{i=1}^{n} k_{it}\right)^{\frac{1}{2}}$$

where f_{nt} = the natural frequency in translation
        f_{nr} = the natural frequency in rotation
        m = the isolation platform mass
        n = the number of isolators

$$f_{nr} = \frac{1}{2\pi}\left(\frac{1}{I_r}\sum_{i=1}^{n} r_i^2 k_{ir}\right)^{\frac{1}{2}}$$

k_{it} = the isolator stiffness in translation in the axis of the natural frequency
I_r = the platform moment of inertia about the axis of the natural frequency, with respect to the center of gravity
r_i = the distance of the ith isolator from the center of gravity
k_{ir} = the isolator stiffness in rotation in a direction perpendicular to r_i

Isolation systems must provide protection against excitation from vibration produced within the isolation system. Normally random vibration is produced within the isolation system. For example, in a vibration isolation table used in a laboratory, a blow to the surface of the table produces both an impulse and random vibration. The effect of the random vibration produced within the system is to produce relative motion of the components. This relative motion is given approximately by:

$$X_{RM} = g \left(\frac{1}{32\pi^3} \right)^{\frac{1}{2}} \left(\frac{Q}{f_n^3} \right)^{\frac{1}{2}} PSD^{\frac{1}{2}}$$

where X_{RM} = the maximum relative motion to the excitation within the vibration isolation system
g = the acceleration due to Earth's gravity field (in metric units, 9.81 m/sec^2)
Q = the transmissibility at resonance of the vibration isolation platform
f_n = the fundamental frequency of the vibration isolation platform
PSD = the random vibration excitation (power spectral density) within the vibration isolation system, in units of dimensionless "g^2" per hertz

In applying the above equation it is important to note that the fundamental frequency and Q are for the platform, not the entire vibration isolation system. It is also important to use the proper units: g in the equation has the units of length over time^2, while the PSD is given in units of dimensionless "g^2" per hertz. The relative motion should be in units of length. This equation indicates that the platform used in a vibration isolation system should be very stiff and well damped (low "Q" value). This is exactly the opposite of the optimum characteristics of the entire system, which are low frequency and high "Q".

A system exposed to random vibration vibrates at its fundamental frequency, since random vibration contains all frequencies. The response amplitude of the system is determined by a statistical process. The average or "root-mean-square" amplitude of response of a simple SDOF system exposed to random vibration is given by:[47]

$$g_{rms} = \left(\frac{\pi}{2} f_n Q PSD \right)^{\frac{1}{2}}$$

where g_{rms} = the "root-mean-square" acceleration response, in dimensionless "g"
Q = the transmissibility at resonance of the system
f_n = the fundamental frequency of the system
PSD = the random vibration excitation (power spectral density) of the system, in units of dimensionless "g^2" per hertz

It is common in vibration engineering to assume that most structural damage is done by the "3-sigma" peak acceleration. The "3-sigma" acceleration is found by multiplying g_{rms} by a factor of 3. The displacement response of the system is given by:

$$\delta = \frac{g_{rms}}{\left(2\pi f_n \right)^2}$$

where δ = the displacement response
f_n = the fundamental frequency of the system

Table 2.4 gives the power spectral density of some representative environments.

TABLE 2.4 Power Spectral Densities (PSDs)

Environment	Frequency f (Hz)	Power Spectral Density (PSD)
Navy warships	1–50	0.001 g^2/Hz
Minimum integrity test	20–1000	0.04 g^2/Hz
(MIL-STD-810E)	1000–2000	–6 dB/octave
Typical aircraft	15–100	0.03 g^2/Hz
	100–300	+4 dB/octave
	300–1000	0.17 g^2/Hz
	≥1000	–3 dB/octave
Thor-Delta launch vehicle	20–200	0.07 g^2/Hz
Titan launch vehicle	10–30	+6 dB/octave
	30–1500	0.13 g^2/Hz
	1500–2000	–6 dB/octave
Ariane launch vehicle	5–150	+6 dB/octave
	150–700	0.04 g^2/Hz
	700–2000	–3 dB/octave
Space shuttle	15–100	+6 dB/octave
(orbiter keel location)	100–400	0.10 g^2/Hz
	400–2000	–6 dB/octave

REFERENCES

1. July 14, 1989. *Environmental Test Methods and Engineeringlines.* MIL-STD-810E.
2. Parker, J.D. and McQuiston, F.C. 1982. *Heating, Ventilating and Air Conditioning,* 2nd. Ed., John Wiley & Sons, New York, NY.
3. Ungar, E.E., Sturz, D.H., and Amick, C.H. July 1990. Vibration control design of high technology facilities, *Sound and Vibration,* Vol. 24, No. 7, 20.
4. Blevins, R.D. 1979. *Formulas for Natural Frequency and Mode Shape,* Van Nostrand Reinhold. Co., New York, NY.
5. Blevins, R.D. 1979. *Formulas for Natural Frequency and Mode Shape,* Van Nostrand Reinhold, New York, NY.
6. Wrigley, W., Hollister, W.M., and Denhard, W.C. 1969. *Gyroscopic Theory, Design, and Instrumentation,* The M.I.T. Press, Cambridge, MA.
7. Lazan, B.J. 1968. *Damping of Materials and Members in Structural Mechanics,* Pergamon Press, New York, NY.
8. Schetky, L.M. and Perkins, J. April 6, 1978. The 'quiet', alloys, *Machine Design,* Vol. 50, No. 8, 202.
9. James, D.W. 1969. High damping materials for engineering applications, *Mater. Sci. Eng.,* Vol. 4. 1.
10. Adams, R.D. 1972. The damping characteristics of certain steels, cast irons and other metals, *J. Sound and Vibration,* Vol. 23, No. 2, 199.
11. Ashby, M.F. 1992. *Materials Selection in Mechanical Design,* Pergamon Press, New York, NY.
12. Levina, Z.M. 1968. Research on the Static Stiffness of Joints in Machine Tools, in *Advances in Machine Tool Design and Research,* S.A. Tobia and F. Koenigs Berger, Eds., Pergamon Press, London, UK.
13. Rivin, E.I. 1988. *Mechanical Design of Robots,* McGraw Hill, New York, NY.
14. Serrurier, M. August 1938. Structural features of the 200-inch telescope for Mt. Palomar observatory, *Civil Eng.,* Vol. 8. No. 8. 524.
15. Moffltt, G.W. 1947. Compensation of Flexure in Range Finders and Sighting Instruments, *J. Optical Soc. Am.,* Vol. 37, 582.
16. King, H.C. 1955. *The History of the Telescope,* Dover Publications, New York, NY.
17. Manly, P.L. 1991. *Unusual Telescopes,* Cambridge University Press, Cambridge, England.

18. Kamm, L.J. 1990. *DesigningCost-Efficient Mechanisms,* McGraw-Hill, New York, NY.

19. Blanding, D.L. 1992. *Principles of Exact Constraint Mechanical Design*, Eastman Kodak Co., Rochester. NY 14650.

20. Hills, D.A., Nowell, D., and Sackfield, A. 1993. *Mechanics of Elastic Contacts,* Butterworth Heinemann .

21. Brewe, D.E. and Hamrock, B.J. October 1977. Simplified Solution for Elliptical-Contact Deformation Between Two Elastic Solids, *J. Lubrication Technol.*, Vol. 99, 485.

22. Braddick, H.J.J. 1963. *The Physics of Experimental Method,* Chapman & Hall, Ltd.

23. Moore, J.H., Davis, C.C., and Coplan, M.A. 1983. *Building Scientific Apparatus,* Addison-Wesley Publishing Co., Reading, MA.

24. Slocum, A.H. April 1992. The Design of Three Groove Kinematic Couplings, *Precision Engineering,* Vol. 14, No. 2, 67.

25. Slocum, A.H. April 1988. Kinematic Coupling for Precision Fixturing - Part I - Formulation of Design Parameters, *Precision Engineering*, Vol. 10, No. 2, 85.

26. Pollard, A.F.C. 1951. *The Kinematical Design of Couplings in Instrument Mechanisms,* Hilger and Watts. Ltd.

27. Bayer, R.G. 1994. *Mechanical Wear Prediction,* Marcel Dekker, Inc., New York.

28. Bayer, R.G., Shalkey, A.T., and Wayson, January 9, 1969. Designing for zero wear, *Machine Design* 142.

29. Trylinski, W. 1971. *Fine Mechanisms and Precision Instruments,* Pergamon Press, Warsaw.

30. Barnes, Jr., W.P. 1966. Some effects of aerospace thermal environments on high-acuity optical systems, *Appl. Optics,* Vol. 5, 701.

31. Ramsay, J.V. 1961. The optical performance of windows with axial temperature gradients, *Optica Acta,* Vol. 8, 169.

32. Kohler, H. and Strahle, F., 1974. Design of Athermal Lens Systems, in *Space Optics.* Thompson, B.J. and Shannon, R.R., Eds., National Academy of Sciences, Washington, D.C.

33. Sparks, M. November 1971. Optical Distortion of Heated Windows in High-Power Laser Systems, *J. Applied Physics,* Vol. 42, No. 12, 5029.

34. Sliusarev, G.G. February 1959. The Influence of Temperature Gradient of Glass of Optical Systems on the Image Produced by the Latter, *Optics and Spectroscopy,* Vol. VI, No. 2, 134.

35. Jamieson, T. H. April 1981. Thermal effects in optical systems, *Optical Eng.,* Vol. 20, No. 2, 156.

36. Wan Lai, et al. 1986. Design Characteristics ofthe 1.56 m Astrometric Telescope and its Usage in Astrometry, in *Astrometric Techniques*, Eichhorm, H. K. and Leacock, R. J., Eds., IAU.

37. Zurmely, G.E. and Hookman, R.A. 1989. Thermal/Optical Test Setup for the Geostationary Operational Environmental Satellite Telescope, *Proc. SPIE 1 167,* 360.

38. Pearson, E. and Stepp, L. 1987. Response of large optical mirrors to thermal distributions, *Proc. SPIE 748,* 164.

39. Pellerin, C.J. et al. 1985. New opportunities for materials selection trade-offs for high precision space mirrors, *Proc. SPIE 542,* 5.

40. Everitt, C.W.F., Davidson, D.E. and Van Patten, R.A. 1986. Cryogenic star-tracking telescope for Gravity Probe B. *Proc. SPE 619,* 89.

41. Erickson, E.F. et al. 1984. All-aluminum optical system for a large cryogenically cooled infrared echel1e spectrometer, *Proc. SPIE 509*, 129.

42. McGlynn, J.B. 1989. Design and development of a rugged airborne scanning optical assembly for a calibrated IR imaging radiometer, *Proc. SPE 1 167,* 183.

43. Lazan, B.J. 1968. *Damping of Materials and Members in Structural Mechanics,* Pergamon Press, Elmsford, NY.

44. Ungar, E.E. 1992. Vibration isolation, in *Noise and Vibration Control Engineering: Principles and Applications,* Beranek, L.L. and Ver, I.L., Eds., John Wiley & Sons, Inc., New York, NY.

45. Vukobratovich, D. 1987. Principles of vibration isolation, Eds., *Proc. SPE 732*, 27.

46. Macinante, J.A. 1984. *Seismic Mounting for Vibration Isolation,* John Wiley & Sons, New York, NY.

47. Harris, C.M. and Crede, C.E. 1976. *Shock and Vibration Handbook,* 2nd. ed., McGraw-Hill Book Co., New York, NY.